

A Family of High-Efficiency Hydrogen-Generation Catalysts Based on Ammonium Species**

Lilin Lu, Haijun Zhang,* Shaowei Zhang,* and Faliang Li

Abstract: Development of highly active, low cost, ecologically friendly, and durable homogenous catalysts for hydrogen generation from hydrolysis of borohydride is one of the most desirable pathways for future hydrogen utilization. The unexpected catalytic activities of inorganic ammonium species and the corresponding mechanisms underpinning them are studied. The catalytic activities of the ammonium species are higher than or comparable to those of mostly investigated noble-metal/transition-metal catalysts (such as Pd, Pt, Ni, and Co) but are considerably cheaper, more environmentally friendly, and more readily available. Quantum chemical calculations indicate that the unique ammonium-induced reaction pathway involved with a barrierless elementary reaction at the reaction entrance and the formation of the highly active intermediate BH_3 are responsible for the unexpected catalytic activities and the significantly accelerated hydrogen generation.

Hydrogen generation from chemical hydride hydrogen storage materials is of great academic and practical importance.^[1–5] Considerable efforts have been made worldwide in hydrogen generation by catalyzed hydrolysis of borohydride under ambient conditions.^[6,7] Catalysts used in these cases were usually noble metals/transition metals, which showed excellent catalytic performances. Unfortunately, they also suffered from several disadvantages, including: 1) low abundance on the earth and high cost; 2) poor catalytic durability due to gradual precipitation and deposition of metaborate reaction products on their surfaces;^[8,9] and 3) detrimental

effects caused by metal residues of the catalysts because almost all of them are usually hazardous to environment. Owing to these disadvantages, metal-free catalysts have recently attracted a great deal of attention and been attempted to catalyze various important reactions. For example, oxidative dehydrogenation and oxygen reduction catalyzed by surface-modified carbon nanotubes, C–H bond activation by boron-doped polymeric carbon nitride and aryl diazonium salts, hydrodefluorination by $[(C_6F_5)_3PF]^+$ cations, and antioxidant synthesis by chiral ammonium hypiodite salts. Catalytic efficiencies of these metal-free catalysts were reported to be higher than or comparable to those of conventional heterogeneous metal catalysts.^[10–17]

Herein, we report, for the first time, the unexpected catalytic activities of inorganic ammonium species, a new family of environmentally friendly and cheap homogeneous metal-free catalysts, in hydrogen generation from the hydrolysis of borohydride and discuss the catalytic mechanisms underpinning it based on quantum chemical calculations. Our results demonstrated that a barrierless elementary reaction induced by the ammonium species and the formation of highly active intermediate BH_3 at the reaction entrance play dominant roles in the catalyzed hydrolysis of borohydride.

We initially investigated the self-hydrolysis of KBH_4 without using any catalyst and the catalytic effects of NH_4Cl , NH_4NO_3 , $(NH_4)_2SO_4$, and NH_4HCO_3 on its hydrolysis at 30 °C (pH 9.7, 10 mL 45 mmol L^{−1} solution of KBH_4 , and 10 mL 0.5 mol L^{−1} ammonium solution; reaction time: 20 min). As expected (Figure 1), the self-hydrolysis rate of KBH_4 was rather low. The amount of H_2 released in 10 min was only about 9.1% of the total theoretical amount.

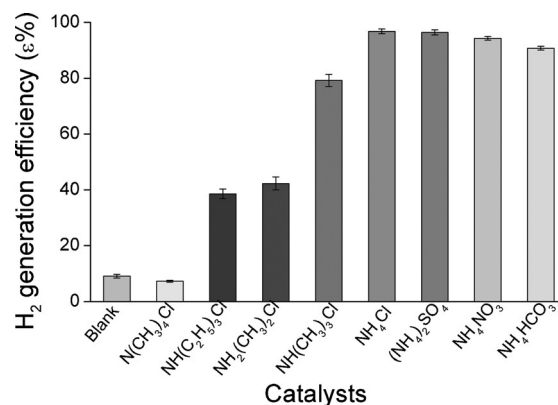


Figure 1. H_2 generation efficiency (ϵ [%]) is the actual volume of released H_2 /maximum theoretical volume of H_2 in the initial 10 min from borohydride hydrolysis catalyzed by different inorganic ammonium species and organic quaternary ammonium species.

[*] L. Lu, H. Zhang, S. Zhang, F. Li
The State Key Laboratory of Refractories and Metallurgy
Wuhan University of Science and Technology
Wuhan 430081 (China)
E-mail: zhanghaijun@wust.edu.cn

L. Lu
College of Chemical Engineering and Technology
Wuhan University of Science and Technology
Wuhan 430081 (China)

S. Zhang
College of Engineering, Mathematics and Physical Sciences
University of Exeter, Exeter EX4 4QF (UK)
E-mail: s.zhang@exeter.ac.uk

[**] This work was financially supported by Natural Science Foundation of Hubei Province of China (2015CFC840), National Natural Science Foundation of China (No. 51472184, 51472185), State Basic Research Development Program of China (973 Program, 2014CB660802), and the fund of State Key Laboratory of Refractories and Metallurgy (G201405).

Supporting information for this article is available on the WWW under <http://dx.doi.org/10.1002/anie.201500942>.

However, upon using NH_4Cl as a catalyst, the hydrolysis rate of KBH_4 increased significantly. H_2 released after only 2 min was already about 70 % of the theoretical amount and reached almost 100 % after 10 min. Similarly to NH_4Cl , NH_4NO_3 , $(\text{NH}_4)_2\text{SO}_4$, and NH_4HCO_3 also showed great catalytic activities which were only very slightly lower than that of NH_4Cl . For NH_4NO_3 and $(\text{NH}_4)_2\text{SO}_4$, such very minor differences might arise from hydrogen bonding interactions existing between NH_4^+ and $\text{NO}_3^-/\text{SO}_4^{2-}$ but not existing between NH_4^+ and Cl^- , and the interactions could slightly inhibit the production of free NH_4^+ ions, thus slightly reducing the catalytic activity in the hydrolysis of KBH_4 . As for NH_4HCO_3 , its relatively low instability in aqueous solution (owing to its self-hydrolysis) might be responsible for the slightly less excellent performance.

The catalytic effect of NH_4Cl on the hydrolysis of KBH_4 was further evaluated under $\text{BH}_4^-:\text{NH}_4^+$ (molar ratio) = 20:1. The results showed that it exhibited an extremely high catalytic activity: 4500 mL- H_2 /min/ g_{catalyst} at 30 °C, which was significantly higher than those of most of the other catalysts reported previously, for example, Ru nanoclusters/zeolite (130 mL- H_2 /min/ g_{catalyst} at 25 °C),^[18] Ru/C (770 mL- H_2 /min/ g_{catalyst} at 25 °C),^[19] Pt-Pd/CNT (126 mL- H_2 /min/ g_{catalyst} at 29 °C),^[20] Pt/LiCoO₂ (3100 mL- H_2 /min/ g_{catalyst} at 22 °C),^[21] and Pt-Ru/LiCoO₂ (2400 mL- H_2 /min/ g_{catalyst} at 25 °C)^[22] (a more comprehensive comparison can be found in the Supporting Information, Table S1). Although the catalytic activity of NH_4Cl is still not so high as that of Pt/C (23 000 mL- H_2 /min/ g_{catalyst}) or Co-B (26 000 mL- H_2 /min/ g_{catalyst}),^[23,24] it should be pointed out that NH_4Cl is respectively 10⁵ and 10³ times cheaper than Pt- and Co-based catalysts. Among the metal-free catalysts, some acids have already proved to be effective catalysts for the hydrolysis of borohydride;^[25] nevertheless, compared to the acid catalysts, ammonium-based catalysts should be more promising especially considering that they are more readily available and cost-effective (NH_4Cl can be readily produced on an industrial scale as the byproduct of the well-known Hou's process for soda production: $\text{NH}_3 + \text{CO}_2 + \text{H}_2\text{O} + \text{NaCl} \rightleftharpoons \text{NH}_4\text{Cl} + \text{NaHCO}_3$). Moreover, as all the investigated inorganic ammonium can be used as nitrogen fertilizer for crops, they are more environmentally friendly than these conventional metal and acid catalysts.

For comparison, the catalytic activities of organic quaternary ammonium salts, for example, triethylammonium chloride ($\text{NH}(\text{CH}_3)_3\text{Cl}$), dimethylammonium chloride ($\text{NH}_2(\text{CH}_3)_2\text{Cl}$), triethylammonium chloride ($\text{NH}(\text{C}_2\text{H}_5)_3\text{Cl}$), and tetramethylammonium chloride ($\text{N}(\text{CH}_3)_4\text{Cl}$), were also evaluated. The results showed that their catalytic activities were, to different extents, lower than those of inorganic ammonium species, and descended in the following order, $\text{NH}(\text{CH}_3)_3\text{Cl} > \text{NH}_2(\text{CH}_3)_2\text{Cl} > \text{NH}(\text{C}_2\text{H}_5)_3\text{Cl} \gg \text{N}(\text{CH}_3)_4\text{Cl} \approx \text{blank}$ (Figure 1; Supporting Information, Figure S1). The catalytic abilities of these quaternary ammonium species are considered to be dependent on their proton-donating capability: the greater this capability, the higher the catalytic activity. It is well-known that the proton-donating capability can be characterized by the dissociation constant K_a . The K_a values of the four quaternary ammonium species investigated increase in the following order: $\text{NH}(\text{C}_2\text{H}_5)_3^+$ ($pK_a = 10.8$) < $\text{NH}_2(\text{CH}_3)_2^+$ ($pK_a = 10.7$) < $\text{NH}(\text{CH}_3)_3^+$ ($pK_a = 9.7$) < NH_4^+ ($pK_a = 9.26$), which is consistent with the order in their catalytic activities. However, $\text{N}(\text{CH}_3)_4^+$ showed almost no catalytic activity in hydrogen generation, which was due to lack of protonic hydrogen in it.

Next, the mechanism of the ammonium-catalyzing reaction was investigated by using the long-range corrected hybrid density functional (wB97XD) with damped atom-atom dispersion corrections with the 6-311++g(2df, 2p) basis set.^[26] The electronic energies of all reactants, intermediates, transition states and products were calibrated based on the couple-cluster theory with single, double and non-iterative triple excitations [CCSD(T)]^[27] with the complete basis set extrapolations,^[28,29] and the solvent effect was also taken into account using the polarizable continuum model with the integral equation formalism (IEFPCM)^[30] to ensure reliability and validity of the results (see the Supporting Information and Table S2 for more details on the calculation procedures). The main results and conclusions based on the wB97XD energetic profiles (Figure 2a) can be summarized as follows. First, BH_4^- anions and NH_4^+ cations can react directly to

The mechanism of the ammonium-catalyzing reaction was investigated by using the long-range corrected hybrid density functional (wB97XD) with damped atom-atom dispersion corrections with the 6-311++g(2df, 2p) basis set.^[26] The electronic energies of all reactants, intermediates, transition states and products were calibrated based on the couple-cluster theory with single, double and non-iterative triple excitations [CCSD(T)]^[27] with the complete basis set extrapolations,^[28,29] and the solvent effect was also taken into account using the polarizable continuum model with the integral equation formalism (IEFPCM)^[30] to ensure reliability and validity of the results (see the Supporting Information and Table S2 for more details on the calculation procedures). The main results and conclusions based on the wB97XD energetic profiles (Figure 2a) can be summarized as follows. First, BH_4^- anions and NH_4^+ cations can react directly to

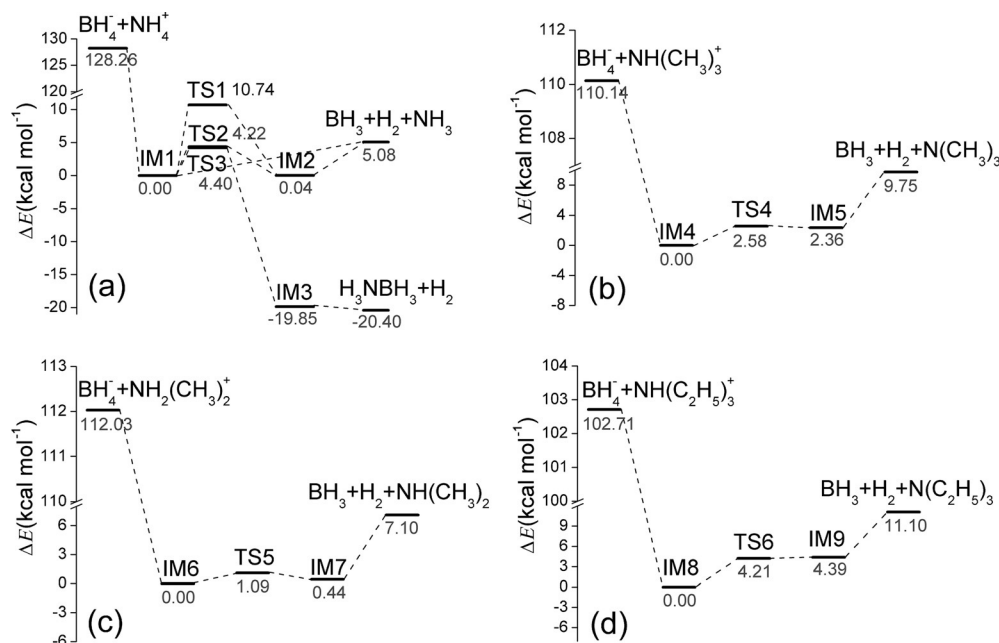


Figure 2. The wB97XD/6-311++g(2df,2p) calculated energetic profiles for the first elementary step in the borohydride hydrolysis catalyzed by a) NH_4^+ and b)–d) organic quaternary ammonium ions.

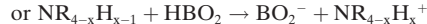
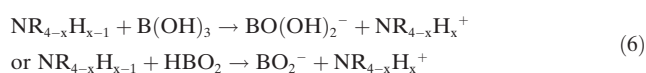
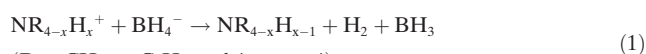
produce a product-like complex of BH_3 , H_2 , and NH_3 , which subsequently dissociates into H_2 and active BH_3 , indicating that the formation of the product-like complex from BH_4^- and NH_4^+ is essentially barrierless. It is worth noting that this barrierless reaction is highly exothermic, with the reaction energy of about $128.26 \text{ kcal mol}^{-1}$, with respect to the initial reactants; this may facilitate the dissociation of the product-like complex and thus the hydrogen release. Second, three transition states, TS1, TS2, and TS3, exist in the reaction pathway between BH_4^- and NH_4^+ . Intrinsic reaction coordinate (IRC)^[31] analysis confirms that TS1 and TS2 are respectively hydrogen exchange transition states between BH_4^- and NH_4^+ , and between H_2 and BH_3 , and TS3 is the transition state producing ammonia borane from the product-like complex of BH_3 , H_2 and NH_3 . The barrier heights of the three reactions (TS1, TS2 and TS3) are 10.74, 4.22, and $4.40 \text{ kcal mol}^{-1}$, respectively. All of the above results suggest that from a kinetic perspective the barrierless reaction between BH_4^- and NH_4^+ is the dominant pathway for H_2 -releasing. Third, the active BH_3 hydrolyzes, forming successively BH_2OH , $\text{BH}(\text{OH})_2$, and $\text{B}(\text{OH})_3$ intermediates, and finally $\text{B}(\text{OH})_3$ dehydrates to BO_2^- species via a four-step reaction (the calculated energetic profiles are presented in the Supporting Information, Figure S2). The barrier heights for the transition states TS1s (from BH_3 to BH_2OH), TS2s (from BH_2OH to $\text{BH}(\text{OH})_2$), and TS3s (from $\text{BH}(\text{OH})_2$ to $\text{B}(\text{OH})_3$) are 21.17, 26.66, and $40.23 \text{ kcal mol}^{-1}$, respectively. Since the reaction pathway is involved with barrierless and low-barrier elementary steps, BH_4^- can hydrolyze easily in the presence of NH_4^+ to release hydrogen.

Furthermore, the catalytic mechanisms of other quaternary ammonium species, such as $\text{NH}(\text{CH}_3)_3^+$, $\text{NH}_2(\text{CH}_3)_2^+$, and $\text{NH}(\text{C}_2\text{H}_5)_3^+$ were investigated (Figure 2b–d). Unlike the inorganic ammonium species, these organic quaternary ammonium cations initially bind with the borohydride anions, forming a stable pre-reactive complex with a binding energy $> 100 \text{ kcal mol}^{-1}$. Next, this pre-reactive complex transforms into a product-like complex of BH_3 , H_2 and corresponding substituted amine (Figures 2b–d) via transition states TS4, TS5 and TS6 with barrier heights of 2.58, 1.09 and $4.21 \text{ kcal mol}^{-1}$, respectively. The low barrier heights suggest that these quaternary ammonium species can react with BH_4^- to produce active intermediate BH_3 , and then accelerate the hydrolysis of borohydride.

The calculated barrier height for the first elementary step catalyzed by each of these quaternary ammonium species is in the following descending order: $E^\ddagger(\text{NH}(\text{C}_2\text{H}_5)_3^+) > E^\ddagger(\text{NH}(\text{CH}_3)_3^+) > E^\ddagger(\text{NH}_2(\text{CH}_3)_2^+)$, which is consistent with the order of their calculated proton affinities (PAs): $\text{N}(\text{C}_2\text{H}_5)_3 > \text{N}(\text{CH}_3)_3 > \text{NH}(\text{CH}_3)_2$: $236.10 > 227.31 > 222.78 \text{ kcal mol}^{-1}$. These calculation results also confirm that the catalytic activities of the

quaternary ammonium species are dominated by their proton-donating capacities. However, the experimental results showed that the catalytic activities of these quaternary ammonium species decrease in the order $\text{NH}(\text{CH}_3)_3^+ > \text{NH}_2(\text{CH}_3)_2^+ > \text{NH}(\text{C}_2\text{H}_5)_3^+$, which is slightly different from that predicted theoretically ($\text{NH}_2(\text{CH}_3)_2^+ > \text{NH}(\text{CH}_3)_3^+ > \text{NH}(\text{C}_2\text{H}_5)_3^+$). This might be attributable to the interplay between electronic effects, steric effects of substituent groups, and solvation effects, which usually have remarkable influence on their proton-donating capacities. However, it is normally difficult to fully take into account the interplay of these effects in the theoretical calculations.

Based on the above theoretical calculations, the hydrolysis process of borohydride catalyzed by $\text{NR}_{4-x}\text{H}_x^+$ can be summarized as follows:



The overall reaction is $\text{BH}_4^- + 3\text{H}_2\text{O} \rightarrow \text{BO}(\text{OH})_2^- + 4\text{H}_2$ or $\text{BH}_4^- + 2\text{H}_2\text{O} \rightarrow \text{BO}_2^- + 4\text{H}_2$. The optimized geometries of all the intermediates and transition states are given in the Supporting Information, Figure S3 and Figure S4, and the proposed reaction pathway for the ammonium-catalyzed hydrolysis of borohydride is illustrated in Figure 3a.

The self-hydrolysis mechanism of BH_4^- was also theoretically studied and compared with that of the ammonium-catalyzed reaction. The results reveal that the borohydride undergoes a stepwise hydrolysis process associated with various intermediates (Supporting Information, Figure S5), and the successive reaction process can be indicated as:

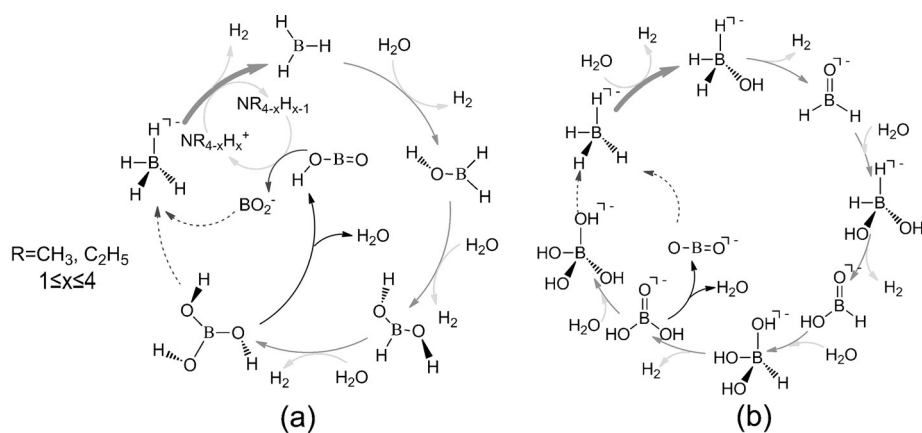


Figure 3. Reaction pathways proposed for hydrolysis of borohydride based on quantum chemical calculations. a) ammonium-catalyzed hydrolysis of borohydride, b) self-hydrolysis of borohydride.

$\text{BH}_4^- \rightarrow \text{BH}_3\text{OH}^- \rightarrow \text{H}_2\text{BO}^- \rightarrow \text{BH}_2(\text{OH})_2^- \rightarrow \text{HB}(\text{O})\text{OH}^- \rightarrow \text{BH}(\text{OH})_3^- \rightarrow \text{B}(\text{O})(\text{OH})_2^- \rightarrow \text{B}(\text{OH})_4^-$ or BO_2^- . It was also found that the self-hydrolysis reaction starts with the formation of pre-reactive complex of BH_4^- and H_2O , then the first intermediate BH_3OH^- and the first H_2 are produced via the transition state TS5s with the highest barrier height of $57.2 \text{ kcal mol}^{-1}$ among all the stepwise reactions. Following this, H_2 elimination reactions and hydration reactions occur alternatively for three times to produce the final products of $\text{B}(\text{OH})_4^-$ or BO_2^- and the other three H_2 molecules (Figure 3b); the calculated energetic profiles and the optimized geometries of intermediates and transition states are given in the Supporting Information, Figures S5 and S6). Based on the above results, the first elementary reaction (from BH_4^- to BH_3OH^-) can be identified as the rate-determining step in the self-hydrolysis of borohydride, and the considerably high barrier height at the reaction entrance is considered to be responsible for the rather delayed hydrogen generation in the case of self-hydrolysis of borohydride.

The reaction pathways given in Figure 3 suggest that the proton-containing ammonium species induce a completely different hydrolysis reaction pathway from that in the self-hydrolysis of BH_4^- . In the ammonium-catalyzed hydrolysis reactions, the barrierless/low-barrier first elementary step and the formation of the highly active intermediate BH_3 associated with the first elementary step result in significant acceleration in the hydrolysis of BH_4^- .

The effects of other factors on the catalytic activity of NH_4Cl in the KBH_4 hydrolysis were also investigated. The concentration of NH_4Cl showed some positive influence on the hydrogen-generating efficiency, and a higher ammonium concentration leads to a higher reaction rate and more hydrogen generation (Supporting Information, Figure S7). Nevertheless, no linear dependence of hydrogen-generating efficiency on the KBH_4 concentration was found (Supporting Information, Figure S8). The highest hydrogen generation efficiency was obtained herein when a 4.50 mmol L^{-1} KBH_4 solution was used (Supporting Information, Figure S9). Furthermore, pH was found to have some effect. A low pH was more favorable for the hydrogen generation catalyzed by NH_4Cl ; however, the difference was not very evident over the pH range from 9.70 to 12.10 (Supporting Information, Figure S10). Upon increasing the pH to 13.10, the catalytic efficiency of NH_4Cl decreased remarkably, this could be attributed to the occurrence of the reaction between OH^- and NH_4^+ , which might suppress the reaction between BH_4^- and NH_4^+ .

The kinetic analysis further confirmed that NH_4Cl -catalyzed hydrolysis reaction was first-order with respect to the initial KBH_4 concentration (Supporting Information, Figure S11), and 0.5th order with respect to the initial NH_4Cl concentration (Supporting Information, Figure S12). The hydrogen-generating rate and the total volume of hydrogen generated increased monotonically with the reaction temperature (Supporting Information, Figure S13). From the plot of $\ln(k)$ versus $1/T$, the apparent activation energy of the NH_4Cl -catalyzed hydrolysis of KBH_4 can be determined as $29.3 \pm 3.3 \text{ kJ mol}^{-1}$ (Supporting Information, Figure S14). This value is lower than those in the most cases using conventional noble

and transition-metal catalysts (a detailed comparison is presented in the Supporting Information, Table S3), which further suggests that NH_4Cl is an excellent catalyst for the hydrolysis of KBH_4 .

Investigations on the catalytic durability of NH_4Cl demonstrated that about 60 % of the initial catalytic activity was still retained even after five cycles (Supporting Information, Figure S15). According to the theoretical calculations, NH_4^+ reacts with BH_4^- producing NH_3 in the first step [Eq. (1)], and NH_4^+ could be re-formed via proton-transfer reaction between $\text{B}(\text{OH})_3/\text{HBO}_2$ and NH_3 in the final step [Eq. (6)]. Thus, the proton transfer reaction is key to the durability of ammonium catalysts. Unfortunately, since $\text{B}(\text{OH})_3$ and HBO_2 (pK_a , 9.24) are weak acids and their pK_a values are comparable to that of NH_4^+ (pK_a , 9.26), the formation of NH_4^+ via the proton transfer reaction between $\text{B}(\text{OH})_3/\text{HBO}_2$ and NH_3 may not be efficiently enough, resulting in the gradual deactivation of NH_4Cl .

In summary, we demonstrate for the first time that ammonium species can be used as highly promising catalysts for hydrogen generation from the hydrolysis of KBH_4 . The catalytic activity is as high as approximately $4500 \text{ mL-H}_2/\text{min g}^{-1}$ catalyst at 30°C , which is higher than or comparable to those in the cases using conventional noble or transition-metal catalysts. The apparent activation energy of ammonium-catalyzed hydrolysis reaction is about 29.3 kJ mol^{-1} , which is also lower than those in the most cases using conventional noble or transition-metal catalysts investigated previously. The quantum chemical calculations suggest that the highly active intermediate BH_3 forms from a barrierless reaction between NH_4^+ and BH_4^- , which remarkably accelerates the hydrolysis of borohydride. It is believed that ammonium species would be potentially used as next-generation high-efficiency catalysts for future hydrogen production from hydrolysis of borohydride, thanks to their high catalytic activities demonstrated in this work as well as their low cost and environmental friendliness.

Experimental Section

The hydrolysis tests were performed by mixing a fresh aqueous solution of potassium borohydride (45 mmol L^{-1} , 10 mL) and ammonium solution (0.5 mol L^{-1} , 10 mL) under ambient conditions (30°C , pH 9.7). The H_2 generation efficiency (ϵ [%]) was calculated as the ratio of the volume of H_2 actually released in a given time period to the theoretically expected maximum volume calculated based on the ideal gas equation ($V = nRT/P$). The hydrogen generation rate (HGR [mL s^{-1}]) was determined in terms of the slope of the hydrogen volume–time plot during the initial reaction stage. The purity (ca. 100 %) of produced hydrogen was evaluated by a Gasboard-3100 gas analyzer.

The catalytic mechanism was theoretically studied at the wB97XD/6-311++g(2df,2p) level of theory. The energetic reaction path was confirmed by the IRC method. To ensure reliability of the density functional theory in the calculations of reaction energetic profiles, the energies of all the species were refined using restricted CCSD(T) theory with the complete basis set extrapolations. Dunning's correlation-consistent double, triple, and quadruple basis sets^[32] were used in the extrapolation calculations. For the investigated ammonium ions, the proton-donating capabilities are characterized by proton affinities, which were calculated as the ZPE (zero

point energy)-corrected electronic energy difference between the quaternary ammonium ion and the corresponding amine.^[33]

Keywords: borohydride hydrolysis · catalytic activity · hydrogen generation · ammonium ions · metal-free catalysts

How to cite: *Angew. Chem. Int. Ed.* **2015**, *54*, 9328–9332
Angew. Chem. **2015**, *127*, 9460–9464

- [1] J. Graetz, *Chem. Soc. Rev.* **2009**, *38*, 73–82.
- [2] U. Eberle, M. Felderhoff, F. Schüth, *Angew. Chem. Int. Ed.* **2009**, *48*, 6608–6630; *Angew. Chem.* **2009**, *121*, 6732–6757.
- [3] Z. Han, F. Qiu, R. Eisenberg, P. L. Holland, T. D. Krauss, *Science* **2012**, *338*, 1321–1324.
- [4] R. E. Rodríguez-Lugo, M. Trincado, M. Vogt, F. Tewes, G. Santiso-Quinones, H. Grützmacher, *Nat. Chem.* **2013**, *5*, 342–347.
- [5] M. Yadav, Q. Xu, *Energy Environ. Sci.* **2012**, *5*, 9698–9725.
- [6] D. M. F. Santos, C. A. C. Sequeira, *Renewable Sustainable Energy Rev.* **2011**, *15*, 3980–4001.
- [7] S. S. Muir, X. Yao, *Int. J. Hydrogen Energy* **2011**, *36*, 5983–5997.
- [8] M. Felderhoff, C. Weidenthaler, R. von Helmolt, U. Eberle, *Phys. Chem. Chem. Phys.* **2007**, *9*, 2643–2653.
- [9] Y. Shang, R. Chen, *Energy Fuels* **2006**, *20*, 2142–2148.
- [10] J. Zhang, X. Liu, R. Blume, A. Zhang, R. Schlögl, D. S. Su, *Science* **2008**, *322*, 73–77.
- [11] K. Gong, F. Du, Z. Xia, M. Durstock, L. Dai, *Science* **2009**, *323*, 760–764.
- [12] L. Yang, S. Jiang, Y. Zhao, L. Zhu, S. Chen, X. Z. Wang, Q. Wu, J. Ma, Y. W. Ma, Z. Hu, *Angew. Chem. Int. Ed.* **2011**, *50*, 7132–7135; *Angew. Chem.* **2011**, *123*, 7270–7273.
- [13] Y. Wang, H. Li, J. Yao, X. Wang, M. Antonietti, *Chem. Sci.* **2011**, *2*, 446–450.
- [14] D. P. Hari, P. Schroll, B. König, *J. Am. Chem. Soc.* **2012**, *134*, 2958–2961.
- [15] C. Yuan, Y. Liang, T. Hernandez, A. Berriochoa, K. N. Houk, D. Siegel, *Nature* **2013**, *499*, 192–196.
- [16] C. B. Caputo, L. J. Hounjet, R. Dobrovetsky, D. W. Stephan, *Science* **2013**, *341*, 1374–1377.
- [17] M. Uyanik, H. Hayashi, K. Ishihara, *Science* **2014**, *345*, 291–294.
- [18] M. Zahmakiran, S. Ozkar, *Langmuir* **2009**, *25*, 2667–2678.
- [19] J. S. Zhang, W. N. Delgass, T. S. Fisher, J. P. Gore, *J. Power Sources* **2007**, *164*, 772–781.
- [20] R. Peña-Alonso, A. Sicurelli, E. Callone, G. Carturan, R. Raj, *J. Power Sources* **2007**, *165*, 315–323.
- [21] Y. Kojima, K. Suzuki, K. Fukumoto, M. Sasaki, T. Yamamoto, Y. Kawai, H. Hayashi, *Int. J. Hydrogen Energy* **2002**, *27*, 1029–1034.
- [22] P. Krishnan, T. H. Yang, W. Y. Lee, C. S. Kim, *J. Power Sources* **2005**, *143*, 17–23.
- [23] Y. Bai, C. Wu, F. Wu, B. Yi, *Mater. Lett.* **2006**, *60*, 2236–2239.
- [24] B. H. Liu, Q. Li, *Int. J. Hydrogen Energy* **2008**, *33*, 7385–7391.
- [25] R. E. Davis, C. G. Swain, *J. Am. Chem. Soc.* **1960**, *82*, 5949–5950.
- [26] J. D. Chai, M. Head-Gordon, *Phys. Chem. Chem. Phys.* **2008**, *10*, 6615–6620.
- [27] G. D. Purvis III, R. J. Bartlett, *J. Chem. Phys.* **1982**, *76*, 1910–1918.
- [28] D. Feller, *J. Chem. Phys.* **1992**, *96*, 6104–6114.
- [29] T. Helgaker, W. Klopper, H. Koch, J. Noga, *J. Chem. Phys.* **1997**, *106*, 9639–9646.
- [30] J. Tomasi, B. Mennucci, R. Cammi, *Chem. Rev.* **2005**, *105*, 2999–3093.
- [31] C. Gonzalez, H. B. Schlegel, *J. Phys. Chem.* **1990**, *94*, 5523–5527.
- [32] D. E. Woon, T. H. Dunning, Jr., *J. Phys. Chem.* **1993**, *98*, 1358–1371.
- [33] C. Carlin, M. S. Gordon, *J. Comput. Chem.* **2015**, *36*, 597–600.

Received: February 1, 2015

Revised: May 9, 2015

Published online: June 18, 2015